OSCILLOSCOPE-BASED TCSPC LONGITUDINAL BEAM DIAGNOSTICS AT HLS-II*

Mingdong Ma, Xing Yang, Yongbin Leng†
National Synchrotron Radiation Laboratory,
University of Science and Technology of China, Hefei, China

Abstract

The longitudinal density distribution of electron bunches is a critical parameter for evaluating the performance of storage rings. To meet the requirements for real-time, cost-effective, and flexible longitudinal diagnostics for the Hefei Advanced Light Facility (HALF), we have developed a Time-Correlated Single Photon Counting (TCSPC) measurement system based on a general-purpose high-speed oscilloscope at the Hefei Light Source II (HLS-II). Unlike traditional setups relying on dedicated TCSPC modules, this system utilizes an oscilloscope to directly acquire single-photon pulses from a Photomultiplier Tube (PMT). Experiments conducted at the HLS-II beamline successfully recovered the bunch fill pattern and reconstructed the photon arrival time distribution. To address the measurement errors caused by amplitude fluctuations, a post-processing algorithm incorporating Software Constant Fraction Discrimination (CFD) and time folding was developed. This approach effectively suppressed the time walk effect and enabled high-resolution reconstruction of the bunch profile. The results demonstrate that this oscilloscope-based scheme possesses excellent online monitoring capabilities, providing a cost-effective technical solution for HALF and similar facilities.

INTRODUCTION

The longitudinal density distribution of electron bunches is a parameter of paramount importance for evaluating beam dynamics in storage rings [1]. For longitudinal diagnostics, dual-sweep streak cameras are traditionally favored due to their sub-picosecond time resolution [2, 3]. However, their inherent deflection scanning mechanisms and limited readout speeds often preclude continuous, real-time online monitoring at the high repetition rates typical of modern accelerators. Furthermore, streak cameras entail prohibitive costs and complex maintenance [4, 5].

As a robust alternative, Time-Correlated Single Photon Counting (TCSPC) offers superior dynamic range, excellent statistical precision, and continuous real-time monitoring capabilities [6-9]. Conventional TCSPC setups rely on photodetectors paired with dedicated Time-to-Digital Converter (TDC) or Time-to-Amplitude Converter (TAC) modules [10]. While these hardware-centric systems process timestamps rapidly, they fundamentally discard the raw analog waveforms. This reliance on fixed, hardware-level signal discrimination restricts the adaptability of the system when confronted with complex and fluctuating beam conditions in accelerator environments.

† Corresponding author (email: mmd@mail.ustc.edu.cn).

To overcome these hardware limitations and fulfill the stringent diagnostic requirements of the future Hefei Advanced Light Facility (HALF) [11], this paper proposes a highly flexible, oscilloscope-based TCSPC system experimentally validated at the Hefei Light Source II (HLS-II). By leveraging a general-purpose, high-bandwidth oscilloscope for direct raw waveform acquisition, the proposed scheme shifts critical signal processing into the software domain. This "software-defined" architecture allows core algorithms, such as Constant Fraction Discrimination (CFD), to be executed dynamically, thereby circumventing the rigid constraints of traditional hardware and providing a cost-effective, adaptable solution for longitudinal beam monitoring.

EXPERIMENTAL SETUP

The experimental apparatus was deployed at the diagnostic beamline of HLS-II, which operates with a revolution frequency of 4.534 MHz. The system architecture is divided into the optical front-end, the detector auxiliary path, and the integrated acquisition and control system.

Optical Front-end

As shown in Fig. 1, synchrotron radiation is generated by the electron beam passing through the B8 bending magnet. The extracted light is directed to an optical table via a series of high-reflectivity mirrors. To ensure high-fidelity imaging, two achromatic doublets with focal lengths of 1000 mm and 400 mm are employed to achieve 1:1 imaging of the radiation source point at a distance of 2800 mm. The use of achromatic lenses effectively sup-presses chromatic aberration from the broadband synchrotron radiation, ensuring the quality of the image spot.

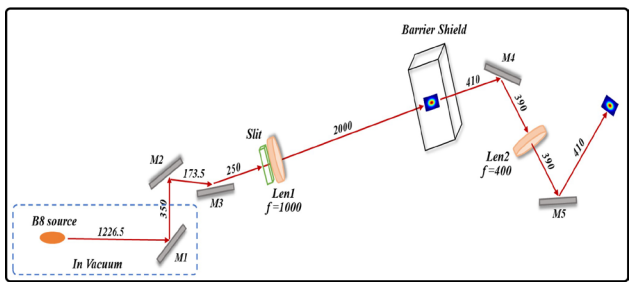

Figure 1: Front-end optical path of the detector.

Detector and Optical Path Conditioning

The layout of the optical table is illustrated in Fig. 2. A high-performance photomultiplier tube (Hamamatsu H10721-110) serves as the photon detector, with its photocathode precisely positioned at the 1:1 imaging point. To ensure the system operates within the single-photon

counting regime and to optimize the signal-to-noise ratio, the following components are placed upstream of the PMT:

Attenuation Module Includes two neutral density (ND) filters (ND 1.0 and ND 3.0) and a motorized six-position filter wheel (Thorlabs FW103) to adjust input intensity based on the beam current.

Wavelength Selection A narrow bandpass filter with a center wavelength of 532 nm and a bandwidth of 10 nm is used to minimize background stray light.

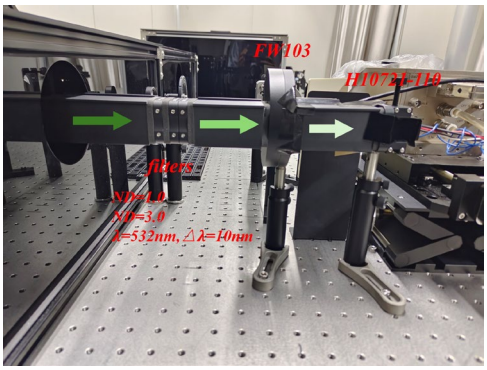

Figure 2: Optical platform layout.

Signal Acquisition and Integrated Control

The signal chain and control logic are shown in Fig. 3. The core of data acquisition is a high-speed digital oscilloscope (Siglent SDS6204 H12 Pro) with a 2 GHz bandwidth and a 10 GS/s sampling rate.

Signal Chain The PMT output is connected to Channel 1 (CH1). For a stable time reference, the revolution frequency signal from the storage ring is processed by a digital delay generator (SRS DG645) for phase adjustment and then fed into Channel 2 (CH2).

Integrated Control A host computer manages the system via standard bus protocols. This includes remote control of the programmable DC power supply (SPD4323X) for PMT gain adjustment, phase control of the reference clock via the DG645, and automated waveform data retrieval from the oscilloscope.

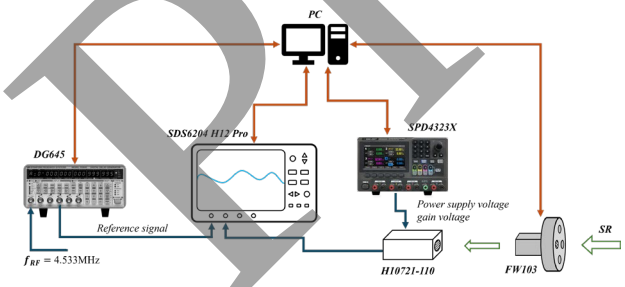

Figure 3: Data acquisition system layout diagram.

DATA ACQUISITION AND SIGNAL POST-PROCESSING

Experimental Conditions

Data acquisition was conducted during HLS-II top-off operation with a beam current of 500 mA. The filling pattern consisted of a long bunch train (35 bunches) and a short bunch train (2 bunches). A total of 400 ms of PMT waveforms and reference signals were recorded for longitudinal profile reconstruction.

Pulse Characteristics and Time Walk Effect

Figure 4 illustrates four typical single-photon pulse waveforms captured by the Photomultiplier Tube (PMT). To provide a clear comparison of the signal features, these pulses are aligned on the time axis using their respective peak points as references. It is evident from the figure that while the timing bases are aligned, the peak voltages of the pulses exhibit significant statistical fluctuations. This phenomenon originates from the fact that the secondary electron emission process within the PMT dynodes follows a Poisson distribution, leading to inherent variations in the amplitude of the resulting electrical signals.

In this context, employing the traditional fixed threshold method for time extraction would cause the relative time at which pulses of different heights cross a given threshold to shift, resulting in the "time walk effect." This artificial timing jitter introduced by amplitude variations directly degrades the resolution of the longitudinal distribution reconstruction, thereby obscuring the true fine structure of the electron bunches.

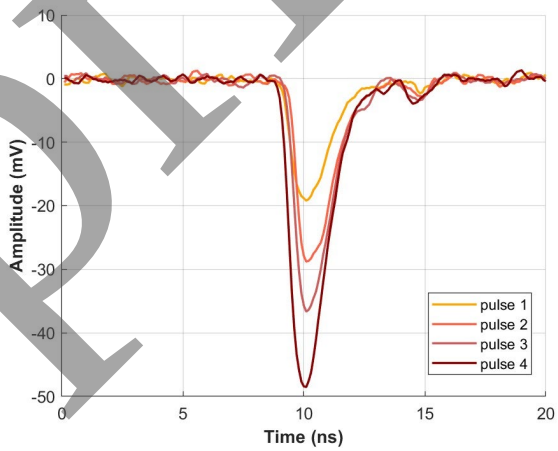

Figure 4: Single photon signals of different amplitudes.

Software CFD and Time Folding Algorithm

To overcome the time walk effect, a software-based Constant Fraction Discrimination (CFD) algorithm was developed for offline processing (Fig. 5):

Pulse Detection The algorithm identifies peak values and times in CH1. Baseline calibration is performed using the pre-pulse region to obtain the true amplitude V_{peak}.

Dynamic Thresholding A constant fraction k (e.g., 50%) is applied to each pulse to calculate a unique threshold ($V_{th} = k * V_{peak}$).

Interpolation Linear interpolation between the two sampling points straddling V_{th} on the leading edge provides the precise photon arrival time.

Synchronization and Folding The algorithm extracts the reference clock from CH2 (the phase-adjusted 4.534 MHz revolution signal). Photon arrival times are calculated relative to this clock edge and folded by the revolution

period to generate a high-resolution longitudinal distribution histogram.

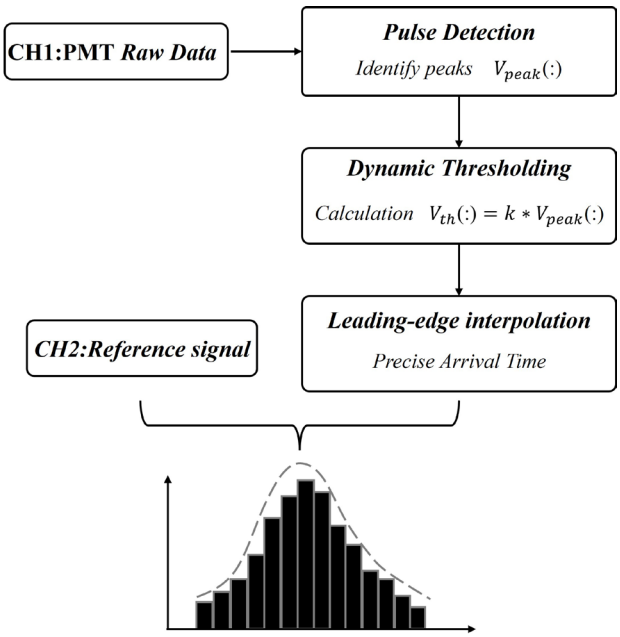

Figure 5: Post-processing data flowchart.

EXPERIMENTAL RESULTS AND DISCUSSIO

Macroscopic Fill Pattern Recovery

By accumulating single-photon events over 400 ms, the system successfully recovered the macroscopic fill pattern of HLS-II. As shown in Fig. 6, the "35+2" structure is clearly visible, comprising a long bunch train of 35 bunches and a short bunch train of 2 bunches. The extremely low counts in the empty buckets demonstrate the system's high dynamic range and signal-to-noise ratio, proving its capability for monitoring bunch charge uniformity and bunch purity.

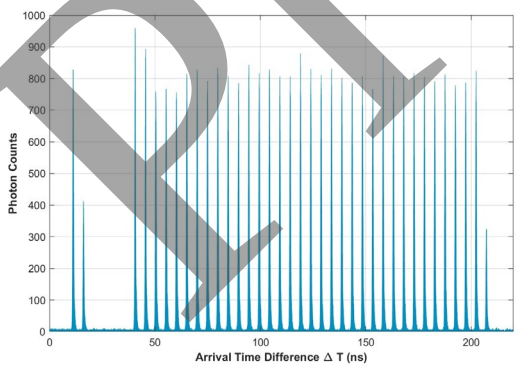

Figure 6: Recovered 35+2 bunch filling pattern at HLS-II.

Microscopic Bunch Profile Measurement

At the microscopic level, the longitudinal density distribution of individual bunches was reconstructed using software CFD and time-folding techniques. Fig. 7 presents the longitudinal distribution of the first bunch within the short bunch train. By applying a Gaussian fit to the experimental data, a standard deviation (σ) of 230.0 ps and a Full Width at Half Maximum (FWHM) of 541.7 ps were obtained.

It should be noted that these measured values represent a convolution of the intrinsic bunch length and the system's Instrument Response Function (IRF). The IRF contribution primarily originates from the PMT transit time spread and the oscilloscope trigger jitter. These results characterize the overall resolution of the system prior to deconvolution and provide a solid experimental basis for the subsequent extraction of the intrinsic bunch length.

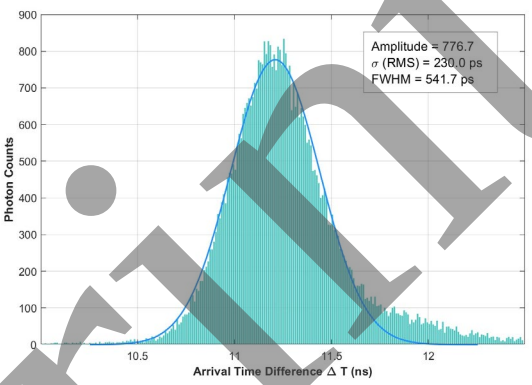

Figure 7: Measured microscopic bunch profile.

CONCLUSION

This study successfully implemented a cost-effective and flexible oscilloscope-based TCSPC longitudinal diagnostics system at HLS-II. By utilizing high-speed direct waveform sampling, the system demonstrates the distinct advantages of a "software-defined" diagnostic approach. Experimental results under top-off operation successfully recovered both the macroscopic fill pattern and the microscopic bunch profiles, with the software CFD algorithm effectively suppressing the time walk effect. Future work will involve further measurement of the system's instrument response function (IRF) to ensure even more accurate measurement results for the upcoming HALF project.

REFERENCES

[1] H.-S. Wang, X. Yang, Y.-B. Leng, Y.-M. Zhou, and J.-G. Wang, "Bunch-length measurement at a bunch-by-bunch rate based on time–frequency-domain joint analysis techniques and its application", *Nucl. Sci. Tech.*, vol. 35, no. 4, 2024. doi:10.1007/s41365-024-01443-z

[2] I. V. Konoplev, G. Doucas, H. Harrison, A. J. Lancaster, and H. Zhang, "Single shot, nondestructive monitor for longitudinal subpicosecond bunch profile measurements with femtosecond resolution", *Phys. Rev. Accel. Beams*, vol. 24, no. 2, Feb. 2021. doi:10.1103/physrevaccelbeams.24.022801

[3] G A Naylor, K Scheidt, J Larsson, M Wulff and J M Filhol, "A sub-picosecond accumulating streak camera for x-rays", *Meas. Sci. Technol.*, vol.12, no. 11, pp. 1858-1864. Oct. 2001. doi:10.1088/0957-0233/12/11/314

[4] Y. K. Zhao *et al.*, "Method for solving bunch head-tail overlapping in HLS-II using a new trigger scanning module of streak-camera measurement system", *ACS Meas. Sci. Au*, vol.

220, p. 113344, Oct. 2023. doi:10.1016/j.measurement.2023.113344

[5] Y. K. Zhao *et al.*, "Application and Development of the Streak Camera Measurement System at HLS-II", in *Proc. IPAC'21*, Campinas, Brazil, May 2021, pp. 1942-1944. doi:10.18429/JACoW-IPAC2021-TUPAB222

[6] V. I. Shcheslavskiy, M. V. Shirmanova, A. Jelzow, and W. Becker, "Multiparametric Time-Correlated Single Photon Counting Luminescence Microscopy", *Biochemistry (Moscow)*, vol. 84, no. S1, pp. 51–68, Jan. 2019. doi:10.1134/s0006297919140049

[7] J. Corbett, P. Leong, and L. Zavala, "Bunch Pattern Measurement via Single Photon Counting at SPEAR3", in *Proc. IBIC'14*, Monterey, CA, USA, Sep. 2014, paper MOPD21, pp. 195-198.

[8] C. A. Thomas, G. Rehm, H. L. Owen, *et al.*, "Bunch purity measurement for Diamond",*Nucl. Instrum. Methods Phys. Res., Sect. A*, vol. 566, no. 2, pp. 762–766, Oct. 2006. doi:10.1016/j.nima.2006.07.059

[9] M. Brosi, J. Schmand, J. Breunlin, and F. Curbis, "Time-Correlated Single-Photon Counting for versatile longitudinal diagnostics at the MAX IV Laboratory storage rings", *Journal of Instrumentation*, vol. 20, no. 03, p. P03011, Mar. 2025. doi:10.1088/1748-0221/20/03/p03011

[10] B. X. Yang, W. E. Norum, S. E. Shoaf, and J. B. Stevens, "Bunch-by-Bunch Diagnostics at the APS Using Time-Correlated Single-Photon Counting Techniques", in *Proc. BIW'10*, Santa Fe, NM, USA, May 2010, paper TUPSM044, pp. 238-242.

[11] A. Wang, Y. Leng, P. Lu, and Y. Yan, "Design Optimization of the HALF Beam Lifetime Measurement System," *IEEE Trans. Nucl. Sci.*, vol. 72, no. 10, pp. 3180–3193, Oct. 2025. doi:10.1109/tns.2025.3611028